ASIAN JOURNAL OF CIVIL ENGINEERING (BUILDING AND HOUSING) VOL. 10, NO. 4 (2009)
PAGES 427-449

BEHAVIOUR OF RESTRAINED SIFCON TWO WAY SLABS PART 1: FLEXURE

H. Sudarsana Rao[*a], N.V. Ramana[b] and K. Gnaneswar[c]
[a]Department of Civil Engineering, JNTU College of Engineering, Anantapur-515002, Andhrapradesh, India
[b]APGENCO, RTPP,Kadapa-516312, Andhrapradesh, India
[c]JNTU College of Engineering, Anantapur-515002, Andhrapradesh, India

ABSTRACT

In this two-part paper, the response of restrained SIFCON two-way slabs is investigated. In part-1, different restrained SIFCON two-way slab specimens were loaded in flexure using the Whiffle-Tree loading arrangement and first crack loads, ultimate loads and load-deflection responses were obtained. In part-2 results from punching shear tests performed on SIFCON two-way slabs are reported. Black steel wire fibres were used in the production of SIFCON slab specimens and the influence of fibre volume percentage on flexural and punching shear behavior is investigated.

In this paper, the influence of volume percentage of steel fibres on strength and stiffness characteristics of slurry infiltrated fibrous concrete (SIFCON) slabs is investigated by testing nine numbers of SIFCON slabs under flexural loading. In order to compare the results, three numbers of fibre reinforced concrete (FRC) slabs and three numbers of plain cement concrete (PCC) slabs are taken as control specimens. The test results indicate that the SIFCON slabs exhibit high strength, high energy absorption and more ductility characteristics compared to the control specimens. SIFCON slabs with higher fibre volume fraction(12%fibre volume) exhibit superior performance among other slab specimens. Analysing the crack patterns noticed in the experimentation, yield line analysis has been performed and the bending moment coefficients for SIFCON slabs are calculated.

Keywords: sifcon, frc, pcc, slabs, energy absorption, ductility factor

1. INTRODUCTION

Modern structural requirements demand materials with increasingly improved properties such as strength, stiffness, impact and abrasion resistance. Fibre reinforced concretes prepared with different types of fibres have found many structural applications. However, the ductility of fibre reinforced concrete basically depends on the volume fraction of fibres

[*] E-mail address of the corresponding author: hanchate123@yahoo.co.in (H. Sudarsana Rao)

used in the production though various other factors such as type of fibre, its aspect ratio and tensile strength of fibre can also influence the ductility. Efforts have been made to incorporate fibres up to 6% but were affected by difficulties in placing and mixing. Special production methodologies developed in the modern days to overcome this difficulty have lead to the development of another high performance material called as slurry infiltrated fibrous concrete (SIFCON). Slurry infiltrated fibrous concrete (SIFCON) is relatively new material that differs from conventional fibre reinforced concrete (FRC) in terms of production and composition [1, 2]. In SIFCON the fibres are placed fully in the mould to its capacity to form a network and then fibre network is infiltrated by cement-based slurry. The method of fabrication facilitates high volume fraction of fibres that range from 4 to 25 percent, and it is a function of several parameters, including aspect ratio of the fibres, shape, diameter, orientation of fibres, method of packing, mold size etc. This slurry-based matrix must consist of fine particles to infiltrate the fibre network. Slab elements made of such high performance material can have many energy absorbing applications.

Ghalib[3] proposed a design method based on ultimate strength criteria for steel fibre reinforced concrete slabs. Parameswaran et.al.[4] studied the behaviour of high volume(8%) percentage steel fibre mortar specimens subjected to flexure and reported that the specimens possess a flexural strength of above 40 MPa. Kumar et.al.[5] analysed the rectangular RCC slabs for different boundary conditions with corner openings by using yield line theory. Craig et.al. [6] proposed design recommendations and guide lines for one way concrete slab, reinforced with fibre reinforced plastic. Marzouk et.al.[7] investigated the effect of using high strength concrete slabs on the structural behaviour of slab-column connection and reported that high strength slab has a significant effect on the load-deflection characteristics for specimen subjected to high moment. Aron zaslavsky[8] presented yield line analysis for simply supported rectangular concrete slabs with central rectangular openings under uniformly distributed loading. Ali and Kajid Afshari [9] studied the influence of length and volumetric percentage of steel fibres on energy absorption of concrete slabs with various concrete strengths under flexure and the results indicate that longer fibres and high fibre content provide higher energy absorption. Rao and Ramana [10] studied the behaviour of slurry infiltrated fibrous concrete (SIFCON) simply supported two way slabs in flexure. Redzuan Abdullah and Samuel Easterling [11] presented details for a new elemental test method for composite slab specimens under bending. Muttoni and Fernandez Ruiz [12] reported that cracking in reinforced tensile members is highly influenced by the loading history because of the irreversible non-linear behavior of bond and of tensile response of concrete, resulting into residual cracks of non-negligible width and presented a physical model describing it. From the above literature review, it is observed that a little information is available on behaviour of SIFCON slabs. The behaviour under flexure is most important aspect for slabs because in most of the practical applications they have to resist various flexural loads. The objective of this research is to experimentally determine flexural strength, load-deflection response, energy absorption and ductility factors for restrained SIFCON slabs with 8, 10 and 12% fibre volume fraction and to calculate the bending moment coefficients using Yield line theory.

2. EXPERIMENTAL PROGRAM

The experimental program comprises of casting and testing of nine SIFCON slabs, three FRC slabs (2% fibre) and three PCC slabs (M20 grade concrete) clamped on all four edges. The mix proportions of the various slabs are presented in Table 1. All the slabs are square and are of size 600x 600 x 50 mm. The Fixed edge condition has been simulated by placing the slab specimens over the platform and all the top edges of slab specimen are kept under the plates and tightened with nut and bolt system. The details of the loading arrangement are depicted in Figure 1.

Table 1. Mix proportions

S.No	Type of slab	Mix proportion	Volume fraction of fibre	W/C ratio	Dosage of super plasticizer	Mode of vibration
1	SIFCON-8	Cement and sand (1:1 by wt)	8%	0.45	1.5%	Hand tamping
2	SIFCON-10	Cement and sand (1:1 by wt)	10%	0.45	1.5%	Hand tamping
3	SIFCON-12	Cement and sand (1:1 by wt)	12%	0.45	1.5%	Hand tamping
4	FRC-2	Cement, sand and coarse aggregate (1:1.54:3.17)	2%	0.5	-	Table vibration
5	PCC-0	Cement, sand and coarse aggregate (1:1.54:3.17)	No fibres	0.5	-	Table vibration

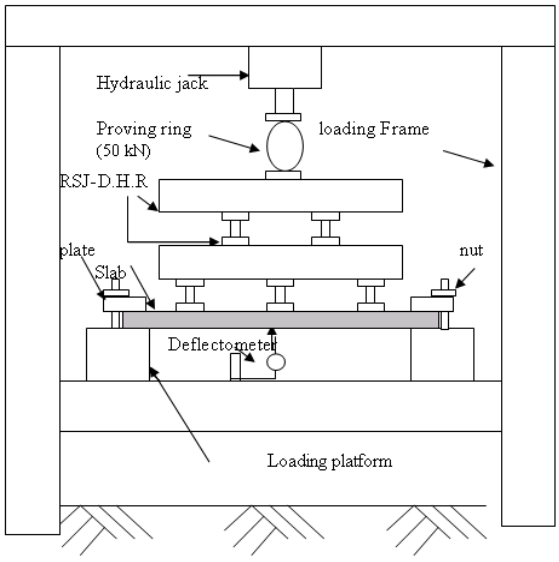

Figure 1. Line diagram of whiffle-Tree loading arrangement

2.1 Materials

2.1.1 Cement

Ordinary Portland cement of 53 grade manufactured by Birla Company confirming to IS 12269 was used. The specific gravity of the cement was 3.01. The initial and final setting times were found as 40 minutes and 340 minutes respectively.

2.1.2 Fine aggregate

Locally available river sand passing through 4.75 mm I S sieve was used. The specific gravity of the sand is found to be 2.62.

2.1.3 Coarse-aggregate

Crushed granite aggregate available from local sources has been used. To obtain a reasonably good grading, 50% of the aggregate passing through 20 mm IS sieve and retained on 12.5 mm IS sieve and 50% of the aggregate passing through 12.5mm IS sieve and retained on 10 mm IS sieve was used in preparation of fibre reinforced concrete and plain concrete slab specimens.

2.1.4 Fibres

The present investigation aims at producing SIFCON with locally available fibres. Accordingly, black annealed steel wire fibres of 1.0 mm diameter were used. The fibres were cut to the required length of 50 mm by using shear cutting equipment giving an aspect ratio of 50. The ultimate tensile strength of fibre was 395 MPa. These black steel wires are commercially available and are generally used for binding the steel reinforcement in RCC works.

2.1.5 Water

PoTable fresh water available from local sources was used for mixing and curing of SIFCON, FRC and PCC slabs.

2.1.6 Super plasticizer

To improve the workability in slurry and concrete, CONPLAST-300 confirming to IS 9103 – 1999 and ASTM C 494 type F high range water-reducing agent has been used.

2.1.7 Casting of test specimens

Steel moulds were used to cast the slab specimens of required size. Two L-shaped frames with a depth of 50 mm were connected to a flat plate at the bottom using nuts and bolts. Cross-stiffeners were provided to the flat plate at the bottom to prevent any possible deflection while casting the specimens. The gaps were effectively sealed by using thin card-boards and wax to prevent any leakage of cement-sand slurry in SIFCON slab specimens. Initially the steel mould was coated with waste oil so that the slab specimens can be removed easily from the moulds. The steel fibres are placed randomly in the mould such that they occupy the entire volume of the mould. In the mean time cement-sand slurry was prepared using CONPLAST-300 which was later poured into the mould uniformly over the

pre-placed fibres. In case of fibre reinforced concrete slabs, fibres were first mixed in the dry mixture of cement and sand and then spread over the heap of coarse aggregate. Hand mixing was done after adding required quantity of water to achieve uniform dispersion of fibres and to prevent the segregation or balling of fibres during mixing. For both FRC and PCC slab specimens, Table vibration was adopted. The test specimens were de-moulded after 24 hrs and were cured for 28 days in curing water ponds. After removing the slab specimens from the curing pond, they were allowed to dry under shade for a while and then they were coated with white paint on both sides, to achieve clear visibility of cracks during testing. The loading position on the top and the dial gauge position at the bottom of the slab were marked with black paint.

To simulate the four edges fixed edge condition, 10mm diameter bolts are welded to the platform at 110mm c/c. A strip of perforated plate of 8mm thick is placed along the four edges of the pre-placed slab such that through the perforations the bolt should come out and get tightened with nuts. This arrangement will arrest the free rotation and displacement at the edge. This can be observed in Figure 2.

Figure 2. Simulation of fixed edge condition using nut and bolt system.

The set up for loading the slab consists of nine numbers of RSJ's (Rolled Steel Joists) of double headed rail of 460 mm length (D.H.R. 130 N/m). These RSJ's were placed over the slab as shown in Figure 2, to obtain the Whiffle-Tree loading arrangement. This arrangement will distribute the centrally applied load from hydraulic jack uniformly on the entire slab and was used by earlier researchers working on RCC slabs [13,14]. The self

weight of these joists was found to be 180Kg and the same has been taken into account in load-deflection computations.

At the bottom face of the slab specimen, a deflectometer with a least count of 0.01 mm was placed at the center to record the deflections. The load was applied through the hydraulic jack with 500 KN capacity proving ring to measure the applied load. The load has been applied in increments of 0.833 KN (1 division of proving ring). Corresponding to each load increment, the central deflection has been recorded. The ultimate load and corresponding deflection at the center were also observed and recorded.

3. DISCUSSION OF TEST RESULTS

3.1 First crack load:-

The first crack loads obtained for different SIFCON, FRC and PCC slab specimens are presented in Table 2. From this Table 2 it can be observed that the SIFCON slab specimens show higher first crack load than the FRC and PCC slab specimens. Among the SIFCON specimens, the specimen SIFCON-12 recorded a first crack load of 27.49 kN, which is the highest among all the slab specimens. This is mainly due to higher volume fraction of fibres present in this slab. The percentage increase of first crack load in SIFCON slab specimens when compared with FRC specimens is in the range of 99 to 119% for different volume fraction of fibres. This confirms the superior performance of SIFCON slab specimens in flexure. The PCC slab specimen does not record any first crack load.

3.2 Ultimate load

The ultimate loads obtained for different SIFCON, FRC and PCC slab specimens are presented in Table 2 and Figure 3. From these, it can be observed that the maximum ultimate load of 94.96kN has been obtained for SIFCON slabs with 12% volume fraction of fibres which is 42% higher than slabs with 8% volume fraction of fibres. This indicates that the ultimate strength of SIFCON slabs increases with increase of fibre content in the ranges tested. The ultimate flexural strength of SIFCON slab specimens are 159 to 267% higher when compared to FRC slab specimens with maximum values corresponding to 12% volume fraction of fibres. The PCC slab specimen has recorded an ultimate load of 7.50kN. The increment when compared to PCC specimens is 788 to 1166%. From this, it is observed that the SIFCON slab specimens behave quite well over the FRC and PCC slab specimens in flexure.

3.3 Load-deflection response

The central deflection values of various slab specimens are presented in Table 2. It can be observed from this Table that the central deflection of SIFCON slab specimens is less when compared to FRC and plain concrete slab specimens at any given load. This is due to the increased stiffness of SIFCON slabs. The maximum deflection of 13.45 mm is observed for SIFCON-12 slab, which is higher than the SIFCON-8 and SIFCON-10 slabs. The SIFCON-8 and SIFCON-10 slabs specimens show a maximum deflection of 22.50mm and 14.70mm respectively. At first crack load, the specimens SIFCON-8, SIFCON-10 and SIFCON-12

show a deflection of 2.48mm, 3.02mm and 3.18mm respectively. The FRC-2 slab shows a deflection of 3.86mm, which is higher than all the SIFCON slab specimens. The load–deflection responses obtained from the present work for all the slab specimens are plotted in Figure 3. From Figure 3, it can be observed that SIFCON slab specimens exhibit greater stiffness at any given load. For example, the stiffness values of all the slab specimens are computed for a deflection of 8mm and are presented in Table 3. It is evident from this Table that SIFCON slabs exhibit greater stiffness than FRC and PCC slab specimens. Among SIFCON slabs, the stiffness increases with increase in percentage of fibres. This increase in stiffness can be attributed to the greater stiffness characteristics of steel wire fibre. Figure 4 presents the load-deflection response in non-dimensional form. This non-dimensional plot has been drawn with δ/δ_c on X-axis and P/P_c on Y-axis, where P is the load at any stage of slab specimen, P_c is the ultimate load of PCC slab, δ is the deflection at any stage corresponding to the load P of slab and δ_c is the ultimate deflection of PCC slab specimen. From this it is observed that the SIFCON-12 shows higher performance than the other slab specimens. This diagram again confirms the superiority of SIFCON slabs over FRC and PCC slab specimens.

The energy absorption for each slab specimen is calculated by integrating the area bounded by the X-axis and load-deflection curve and is presented in Figures 5. The calculated energy absorption of different slab specimens are presented in Table 4. From this it is observed that the SIFCON specimens exhibit higher energy absorption than FRC and PCC slab specimens. Among the SIFCON specimens the SIFCON-12 has recorded the maximum energy absorption of 1426.71 Joules, which is higher than the other two slab specimens i.e. SIFCON-8 (623.98 Joules) and SIFCON-10 (694.86 Joules). The energy absorbing capacity increased with the increase of volume fraction of fibres. The FRC-2 specimen has the energy capacity of 122.34 Joules which is lower than all the SIFCON slab specimens and higher than the PCC slab specimen. The increase of energy absorption capacity of SIFCON specimens is about 410 to 1066% and 9654 to 22202% when compared with FRC-2 and PCC-0 specimens respectively. This increased energy absorption of SIFCON slabs may be mainly due to crack-bridging, crack-deflection and fibre pull-out mechanisms that operate in the specimens. Hence, it can be concluded that the SIFCON slab specimens show superior performance than the FRC and PCC slab specimens in flexure.

Table 2. Maximum central deflection at first crack load and at ultimate load (first cycle)

S.No.	Nomenclature	First crack load (kN)	Maximum central deflection at First crack load (mm)	Ultimate load (kN)	Maximum central deflection at ultimate load (mm)
1.	SIFCON - 8	24.99	2.48	66.64	22.5
2.	SIFCON - 10	26.66	3.02	76.64	14.7

3.	SIFCON - 12	27.49	3.18	94.96	13.45
4.	FRC - 2	12.5	3.86	25.82	8.86
5.	PCC - 0	--	--	7.5	2.2

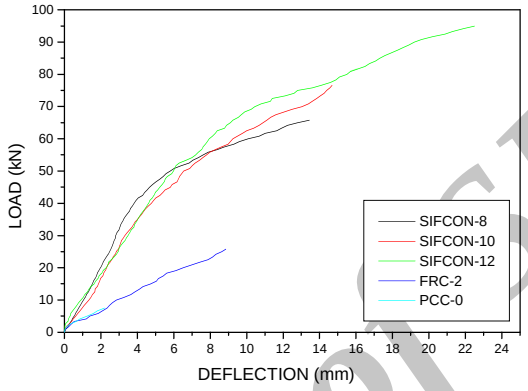

Figure 3. Load-deflection responses of different slab specimens

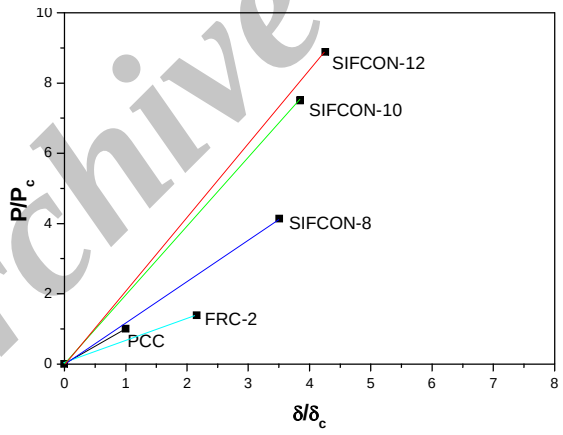

Figure 4. Non dimensional plot of load-deflection response

Table 3. Stiffness of slab specimens

S.No.	Nomenclature	Load at 8mm deflection (kN)	Stiffness at 8mm deflection (kN/mm)

1.	SIFCON -8	56.32	7.04
2.	SIFCON -10	56.32	7.04
3.	SIFCON -12	61.00	7.62
4.	FRC-2	23.63	2.95
5.	PCC-0	--	--

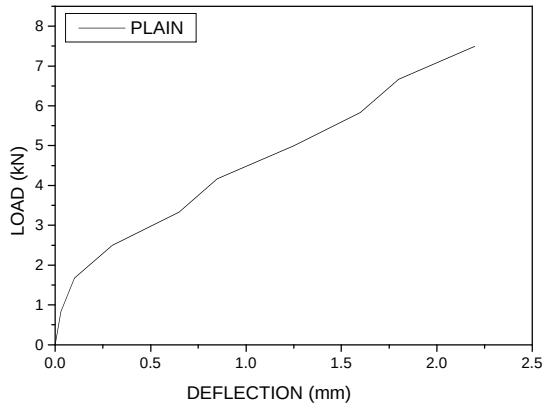

a. Load-deflection curve (PCC-0)

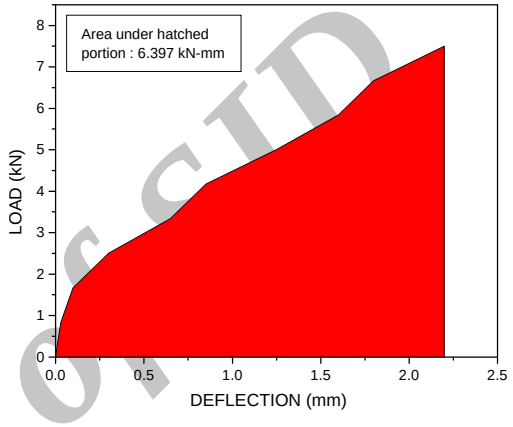

b. Area under load-deflection curve (PCC-0)

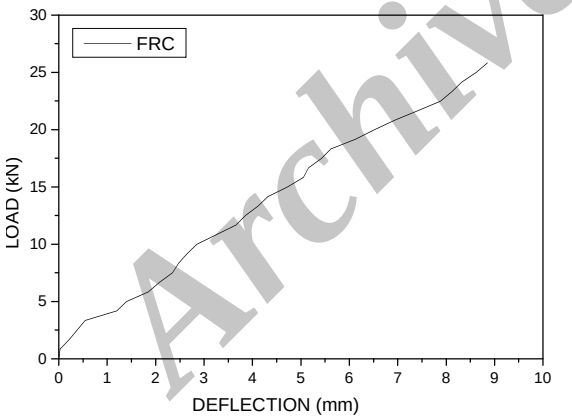

c. Load-deflection curve (FRC-2)

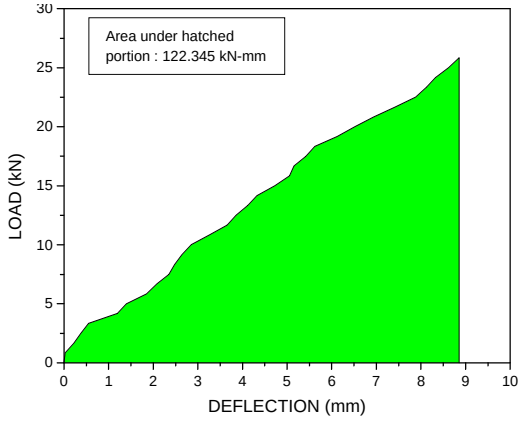

d. Area under load-deflection curve (FRC-2)

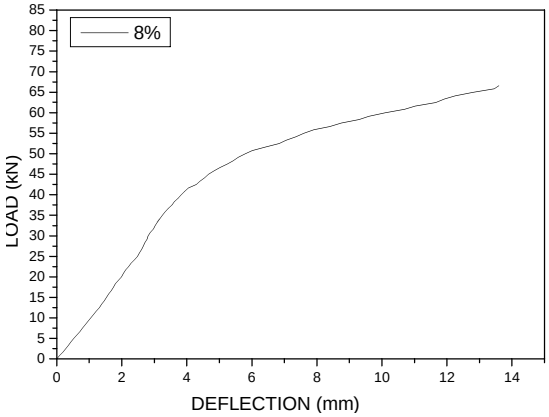

e. Load-deflection curve (SIFCON-8)

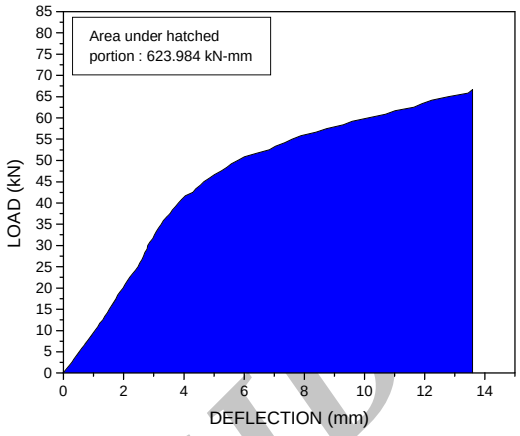

f. Area under load-deflection curve (SIFCON -8)

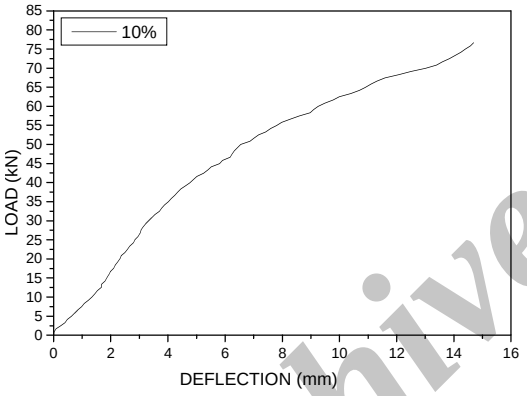

g. Load-deflection curve (SIFCON -10)

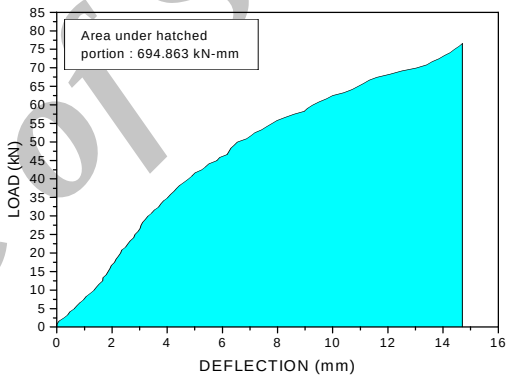

h. Area under load-deflection curve (SIFCON -10)

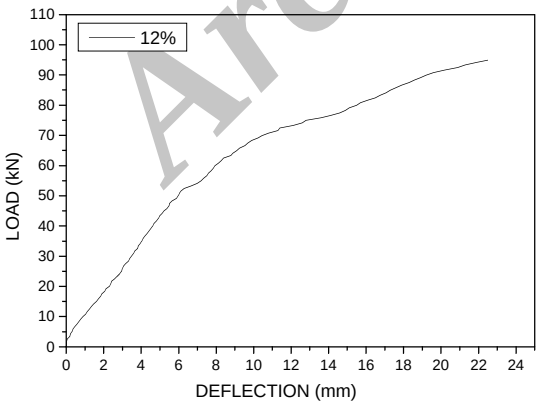

i. Load-deflection curve (SIFCON -12)

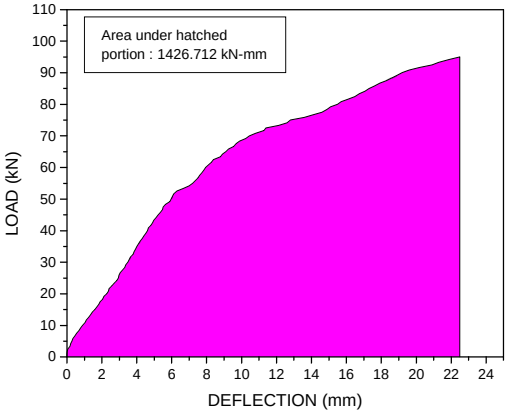

j. Area under load-deflection curve (SIFCON -12)

Figure 5. Energy absorption under first cycle

Table 4. Energy Absorption

S.No.	Nomenclature	Energy absorption (Joules)	% increase w.r.t FRC-2 Slabs	% increase w.r.t. PCC Slabs
1.	SIFCON -8	623.98	410.02	9654.32
2.	SIFCON -10	694.86	467.95	10762.34
3.	SIFCON -12	1426.71	1066.14	22202.83
4.	FRC - 2	122.34	--	1842.54
5.	PCC - 0	6.40	(-)94.77	--

3.4 Cyclic load behaviour

Cyclic load test has been performed on the SIFCON slab specimens by releasing the load after reaching the ultimate stage and re-applying. The cyclic load-deflection curves obtained from the present work are depicted in Figures 6, 7 and 8. The number of cycles has been restricted to five only due to the dial gauge limitations. These load-deflection curves indicate the capacity and the performance of SIFCON slabs to with stand the cyclic loading. A discussion on cyclic load characteristics of SIFCON slabs is presented in following sections.

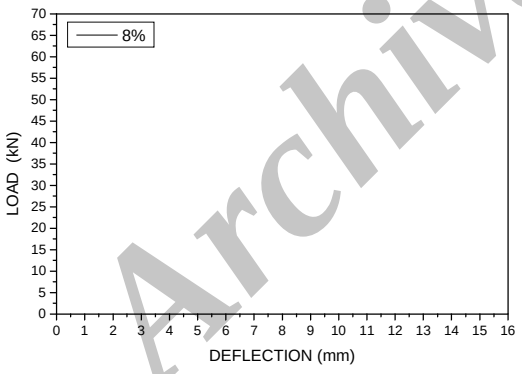

Figure 6. Cyclic load behaviour (SIFCON -8)

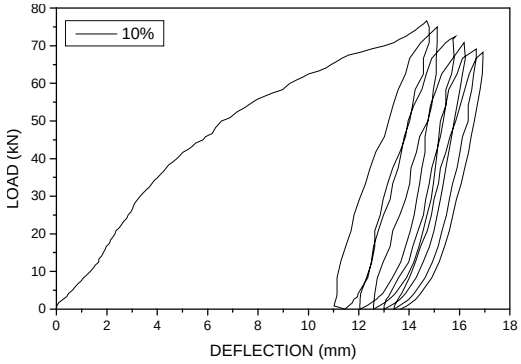

Figure 7. Cyclic load behaviour (SIFCON-10)

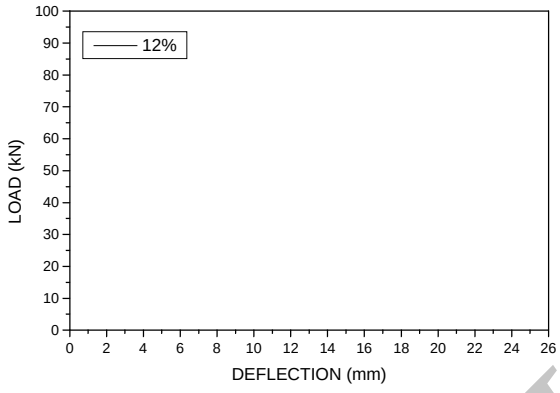

Figure 8. Cyclic load behaviour (SIFCON -12)

3.5 Cyclic ductility characteristics

The ductility factor values for various load cycles of the slab specimens are worked out and are presented in Table 5. The cumulative ductility factor values for various cycles for the slab specimens are also presented in Table 5. The cumulative ductility factor is found to increase from 5.48 to 29.79 for SIFCON-8, 4.87 to 26.00 for SIFCON-10 and 7.08 to 36.26 for SIFCON-12. The FRC and PCC specimens do not show cyclic load performance. The FRC-2 and PCC-0 have the ductility factor of 2.24 and 1.00 respectively. The same values are considered as cumulative ductility factors as they did not exhibit cyclic load behaviour. The effect of cumulative ductility factor vs number of cycles for different slab specimens are presented in Figure 9. From Figure 9, it is observed that as the percentage volume of fibres increases in SIFCON slab specimens, the cumulative ductility factor increases. The cumulative ductility factor increased almost five times for all SIFCON slab specimens from first cycle to fifth cycle. This reveals the enormous energy absorption capacities and very high ductile behaviour of SIFCON two-way slabs. This observation projects SIFCON slab as a potential construction material in earth quake resistant structures.

Table 5. Ductility factors

Nomenclature	Cycle	Deflection at yield load (D_y) (mm)	Deflection at ultimate load (D_u) (mm)	Ductility factor (D_u/D_y)	Cumulative ductility factor
SIFCON -8	1	2.48	13.60	5.48	5.48
	2	2.48	14.62	5.90	11.38
	3	2.48	14.89	6.00	17.38
	4	2.48	1524	6.15	23.53
	5	2.48	15.49	6.25	29.79

SIFCON -10	1	3.02	14.70	4.87	4.87
	2	3.02	15.12	5.01	9.87
	3	3.02	15.84	5.25	15.12
	4	3.02	16.18	5.36	20.48
	5	3.02	16.67	5.52	26.00
SIFCON-12	1	3.18	22.50	7.08	7.08
	2	3.18	22.86	7.19	14.26
	3	3.18	23.25	7.31	21.58
	4	3.18	23.35	7.34	28.92
	5	3.18	23.36	7.35	36.26
FRC-2	1	3.86	8.86	2.24	2.24
PCC-0	1	2.20	2.20	1.00	1.00

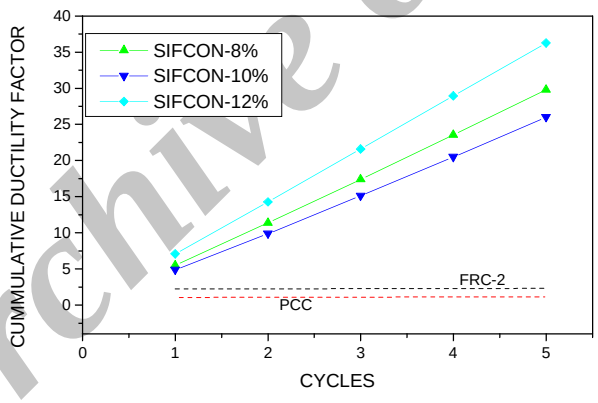

Figure 9. Cumulative ductility factor vs number of cycles

3.6 Cumulative energy absorption capacity

The energy absorption capacities during various load cycles are calculated as the sum of the areas under the hystersis loops from load vs. deflection diagram using integration. The values of cumulative energy absorption capacities obtained from this investigation are presented in Table 6. The variation of cumulative energy absorption with various load cycles is depicted in Figure 10. The cumulative energy absorption for SIFCON-8, SIFCON-10 and SIFCON-12 is about 577 to 786 Joules, 602 to 980 Joules and 1246 to 1720 Joules respectively. From Figure 10 it can be observed that cumulative energy absorption increases with increase in percentage fibre content of SIFCON slabs. The increase is steady from

cycle to cycle. The highest slope of SIFCON-12 specimen indicates that at higher percentages there is a rapid increase in energy absorption capacities of SIFCON slabs. From Table 6 it is observed that the cumulative energy absorption of SIFCON slabs is about 372 to 1306% and 8922 to 26780% higher than the FRC and PCC slab specimens respectively.

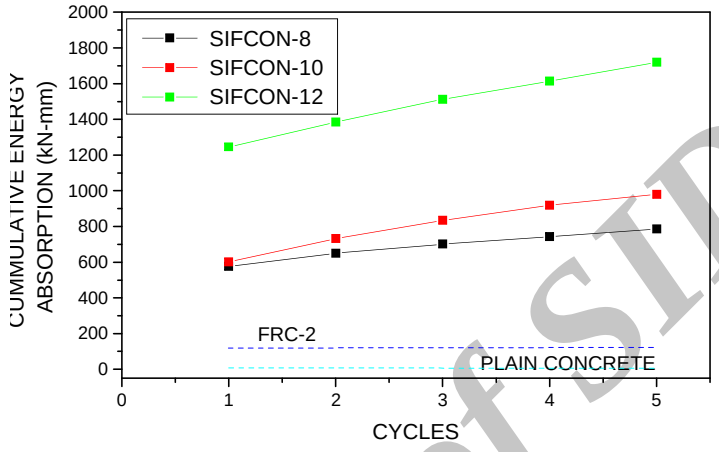

Figure 10. Cumulative energy absorption vs number of cycles

Table 6. Cumulative energy absorption capacities

Nomenclature	Cycle	Energy absorption (Joules)	Cumulative energy absorption (Joules)	% increase of cumulative energy absorption with respect to FRC	% increase of cumulative energy absorption with respect to PCC
SIFCON-8	1	577.45	577.45	372.00	8922.66
	2	73.33	650.78	431.94	10068.44
	3	51.04	701.82	473.66	10865.94
	4	41.83	743.66	507.86	11519.69
	5	43.28	786.93	543.23	12195.78
SIFCON-10	1	602.19	602.19	392.23	9309.22
	2	131.46	733.65	499.68	11363.28
	3	101.37	835.03	582.55	12947.34

	4	84.64	919.67	651.73	14269.84
	5	61.18	980.85	701.74	15225.78
	1	1246.13	1246.13	918.58	19370.78
	2	139.42	1385.56	1032.55	21549.38
SIFCON-12	3	126.99	1512.55	1136.35	23533.59
	4	101.9	1614.45	1219.64	25125.78
	5	105.9	1720.35	1306.20	26780.47
FRC-2	1	122.34	122.34	--	1811.56
PCC-0	1	6.4	6.4	-94.77	--

3.7 Cracking and failure pattern

The crack patterns of different slabs are presented in Figures 11 to 15. It can be observed from Figures 11 to 15 that the crack pattern is almost similar in all the SIFCON Slabs. While conducting the experiment, it is observed that the first crack originated at the edges and with increment of load propagated diagonally towards the corner. The spacing of cracks is observed to decrease with increase in percentage volume of fibres among SIFCON slabs. This is expected because at higher percentage volumes more crack-bridging will take place. The failure of SIFCON slabs is very gradual and the slabs were intact even after ultimate load is reached. After performing the cyclic loading up to five cycles, it is observed that already formed cracks are getting widened with formation of few new cracks. Not many cracks have propagated from bottom face to top face of SIFCON slabs even after five cycles of loading. On the other hand the cracks have appeared on the top surface in case of FRC slabs. In PCC slab specimens the first crack originated at center and with increment of load the crack propagated diagonally towards the corner. The propagation of cracks was observed to be faster in PCC slab specimens and the failure is almost instantaneous, breaking the slab in to pieces. It is depicted in Figure 15. The crack pattern in SIFCON slabs after five cycles of loading consists of four trapeziums and one rectangle. Similar observation can be made even for FRC slab specimens.

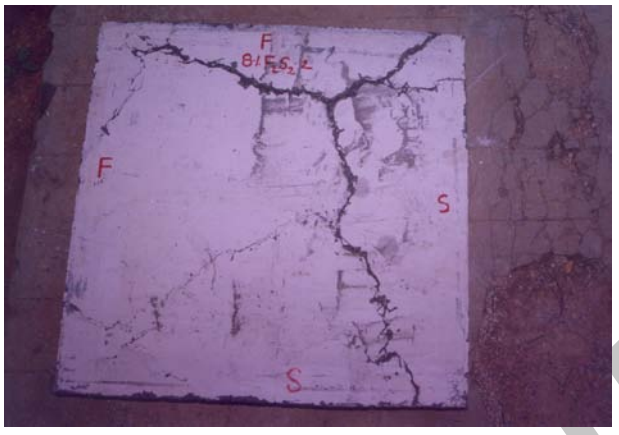

Figure 11. Failed specimen depicting crack pattern of SIFCON-8% fibre volume slab specimen

Figure 12. Failed specimen depicting crack pattern of SIFCON-10% fibre volume slab specimen

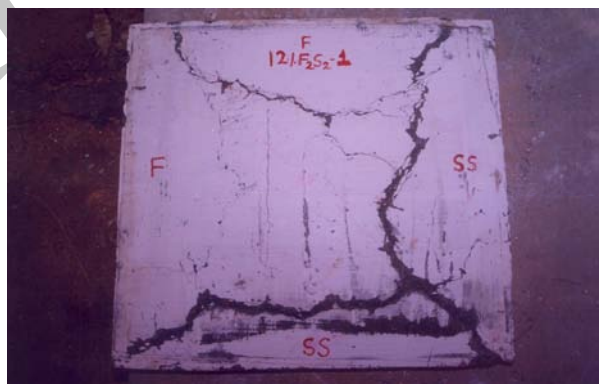

Figure 13. Failed specimen depicting crack pattern of SIFCON-12% fibre volume slab

specimen

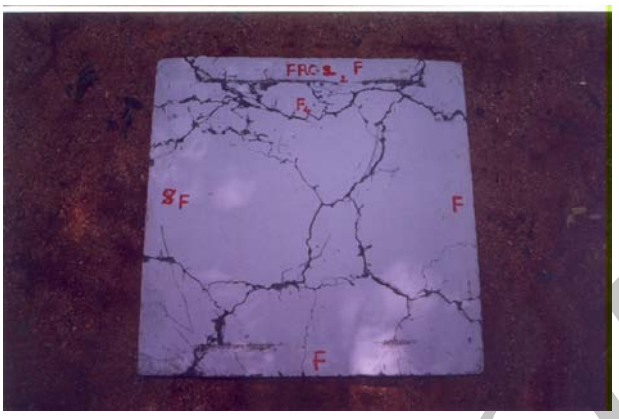

Figure 14. Failed specimen depicting crack pattern of FRC-2% fibre volume slab specimen

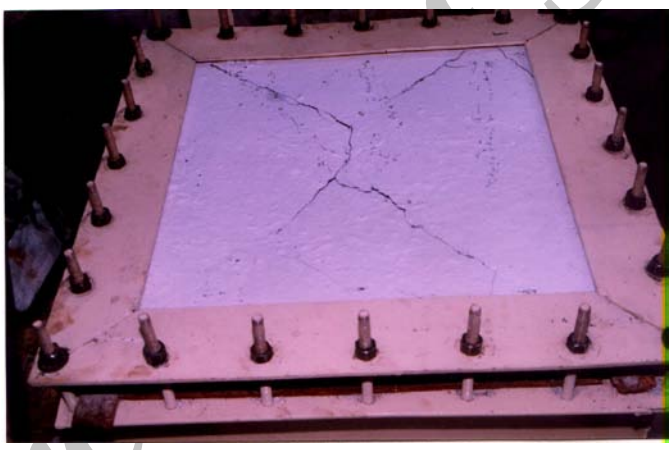

Figure 15. Failed specimen depicting crack pattern of PCC-0 slab

3.8 Determination of bending moment coefficients using Yield line analysis

In I.S 456-2000, bending moment coefficients have been reported for RCC slabs with different edge conditions. The present study aims to calculate bending moment coefficients for restrained SIFCON two-way slabs which can be effectively used to predict the moment capacities of SIFCON slabs. Yield line analysis has been used for this purpose. Figure 16 shows the yield line pattern of two way square slab of size 2a x 2λa, which is restrained along all of its edges. Yield line ABCD divides the slab in to five segments: 1-2-3-4-5. Slab segments 1, 2, 3 and 4 are identical with a shape of trapezium. The segment 5 is in rectangular or square shape with a size of 2αb x 2b. Let the deflection at the intersection of yield lines be 'δ'. The determination of bending moment coefficients by using virtual work method is presented in the following sections.

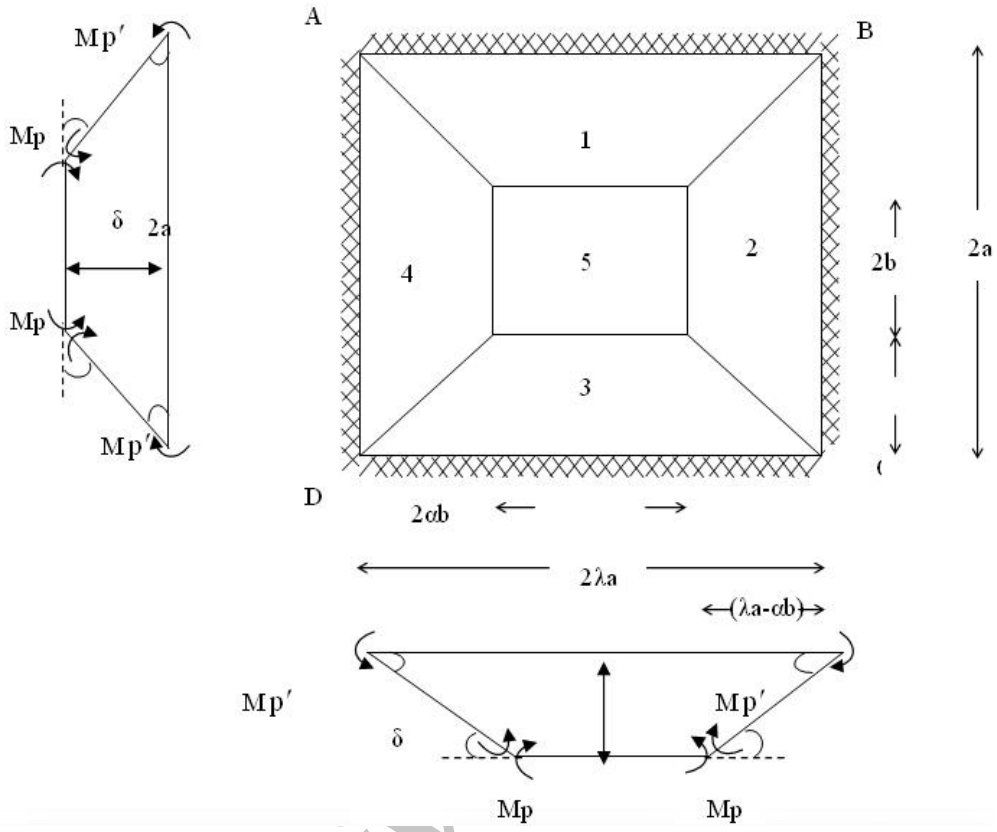

Figure 16. Yield line pattern of slab with all four edges fixed

Internal Work done

$$E = 4Mp(\lambda a - \alpha b)\left(\frac{\delta}{(a-b)}\right) + 4Mp(a-b)\left(\frac{\delta}{(\lambda a-\alpha b)}\right) + 2(2b)Mp\left(\frac{\delta}{(\lambda a-\alpha b)}\right)$$

$$+ 2(2\alpha b)Mp\left(\frac{\delta}{(a-b)}\right) + 2Mp'(2a)\left(\frac{\delta}{(\lambda a-\alpha b)}\right) + 2(2\lambda a)Mp'\left(\frac{\delta}{(a-b)}\right) \quad E = 4Mp\,\delta$$

$$\left[\frac{\lambda a-\alpha b}{(a-b)} + \frac{(a-b)}{(\lambda a-\alpha b)} + \frac{b}{(\lambda a-\alpha b)} + \frac{\alpha b}{a-b} + \frac{Mp'}{Mp}\frac{a}{(\lambda a-\alpha b)} + \frac{Mp'}{Mp}\frac{(\lambda a)}{(a-b)}\right]$$

$$= 4Mp\,\delta\left[\frac{\lambda a}{(a-b)} + \frac{a}{(\lambda a-\alpha b)} + \frac{Mp'}{Mp}\frac{a}{(\lambda a-\alpha b)} + \frac{Mp'}{Mp}\frac{\lambda a}{(a-b)}\right] \quad (1)$$

$$= 4Mp\,\delta\left[\frac{\lambda a}{(a-b)}\left[1+\frac{Mp'}{Mp}\right] + \frac{a}{(\lambda a-\alpha b)}\left[1+\frac{Mp'}{Mp}\right]\right]$$

$$= 4Mp\,\delta\left[\left[1+\frac{Mp'}{Mp}\right]\left[\frac{\lambda a}{(a-b)} + \frac{a}{\lambda a-\alpha b}\right]\right]$$

External Work Done

$$D= w\left[(8)\frac{1}{2}(\lambda a - \alpha b)(a-b)\left(\frac{\delta}{3}\right)+2(2\,\alpha b)(a-b)\left(\frac{\delta}{2}\right)+2(2b)(\lambda a - \alpha b)\left(\frac{\delta}{2}\right)+(2\alpha\, b)(2b)(\delta)\right]$$

$$= \delta w\left[\frac{4}{3}(\lambda a - \alpha b)(a-b) + 2\alpha b(a-b) + 2b(\lambda a - \alpha b) + 4(\alpha b)(b)\right]$$

$$= \frac{2}{3}\delta w[2\lambda a^2-2\alpha ab-2\lambda ab+2\alpha b^2+3\alpha ab-3\alpha b^2+3\lambda ab-3\alpha b^2+6\alpha b^2] \quad (2)$$

$$= \frac{2}{3}\delta w[2\lambda a^2-2\alpha b^2+\alpha ab+\lambda ab]$$

$$= \frac{2}{3}\delta w a^2\left[2\lambda + 2\alpha\,\frac{b^2}{a^2}+\alpha\frac{b}{a}+\lambda\frac{b}{a}\right]$$

$$= \frac{2}{3}\,\delta\, w a^2\left[2\lambda + 2\alpha\,\frac{b^2}{a^2}+(\alpha+\lambda)\frac{b}{a}\right]$$

On equating internal work done and external work done the following equation is obtained to calculate the theoretical bending moment capacity of the section.

$$Mp = \frac{w(2a)^2}{24}\left[\frac{2\lambda+2\alpha\dfrac{b^2}{a^2}+(\alpha+\lambda)\dfrac{b}{a}}{\left(1+\dfrac{Mp'}{Mp}\right)\left[\dfrac{\lambda a}{a-b}+\dfrac{a}{\lambda a-\alpha b}\right]}\right] \quad (3)$$

3.8.1 The Bending moment coefficient for SIFCON-8

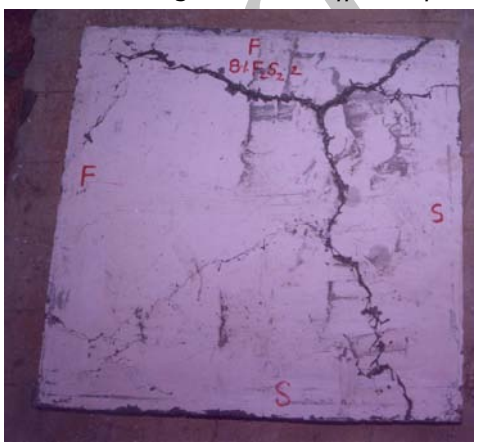

a. Experimental

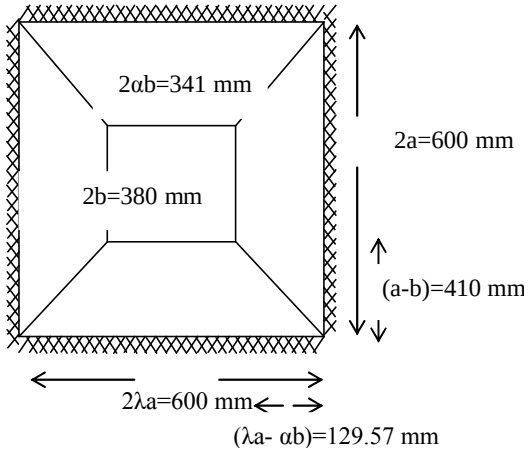

b. Idealized

Figure 17. Yield line pattern(SIFCON-8%)

From equation 3.

$$Mp = \frac{w(2a)^2}{24}\left[\frac{2\lambda + 2\alpha\frac{b^2}{a^2} + (\alpha+\lambda)\frac{b}{a}}{\left(1+\frac{Mp'}{Mp}\right)\left[\frac{\lambda a}{a-b} + \frac{a}{\lambda a - \alpha b}\right]}\right]$$

Note: $Mp = Mp'$

$$= \left[\frac{w(2a)^2}{24}\frac{2\ x1 + 2\,x\,0.897\,x\frac{190^2}{300^2} + 1.897\ x\ \frac{190}{300}}{(2)\left[\frac{1x\ 300}{300-190} + \frac{300}{300-0.897\ x\ 190}\right]}\right] = \frac{w(2a)^2}{24}\left[\frac{3.92}{10.085}\right] = \frac{w(2a)^2}{61.745}$$

$= Mp = 0.0161\ w\ (2a)^2$

$Mp^1 = 0.0161\ w(2a)^2$

Therefore, the bending moment coefficient for SIFCON-8 is 0.0161

3.8.2The bending moment coefficient for SIFCON-10

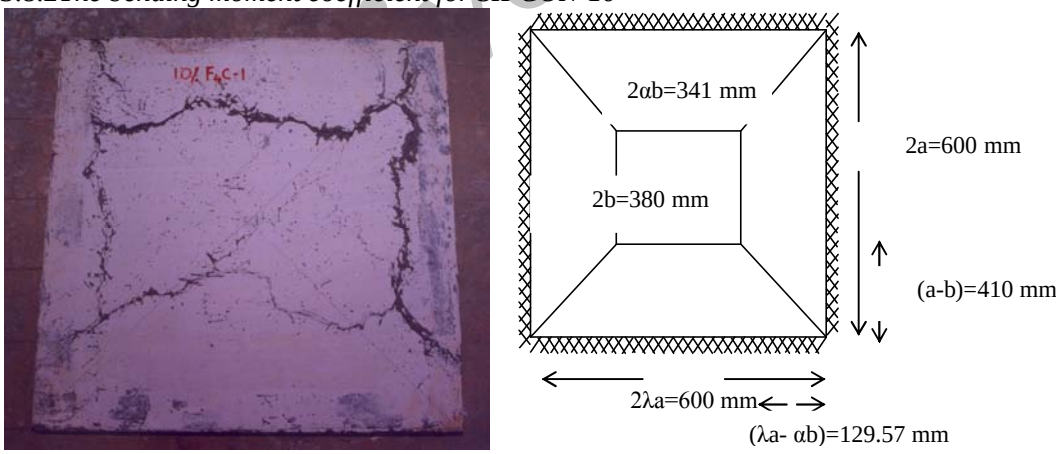

a. Experimental b. Idealized

Figure 18. Yield line pattern (SIFCON-10%)

From the equation 3.

$$Mp = \frac{w(2a)^2}{24}\left[\frac{2\lambda + 2\alpha\frac{b^2}{a^2} + (\alpha+\lambda)\frac{b}{a}}{\left(1+\frac{Mp'}{Mp}\right)\left[\frac{\lambda a}{a-b} + \frac{a}{\lambda a - \alpha b}\right]}\right]$$

Note: $Mp = Mp'$

$$= \frac{w(2a)^2}{24}\left[\frac{2\ x1 + 2\,x1.213\,x\frac{152.5^2}{300^2} + (1.213+1)\ x\ \frac{152.5}{300}}{(1+1)\left[\frac{1x\ 300}{(300-152.5)} + \frac{300}{(1x300 - 1.213x\ 152.5)}\right]}\right]$$

$$= \frac{w(2a)^2}{24}\left[\frac{2 + 0.6268 + 1.125}{(2)(2.033 + 2.6082)}\right]$$

$$= \frac{w(2a)^2}{24}\left[\frac{3.7518}{9.28}\right] = \frac{w(2a)^2}{69.175}$$

$Mp = 0.0168\ w\ (2a)^2$

$Mp' = 0.0168\ w\ (2a)^2$

Therefore, the bending moment coefficient for SIFCON-10 is 0.0168

3.8.3 The bending moment coefficient for SIFCON-12

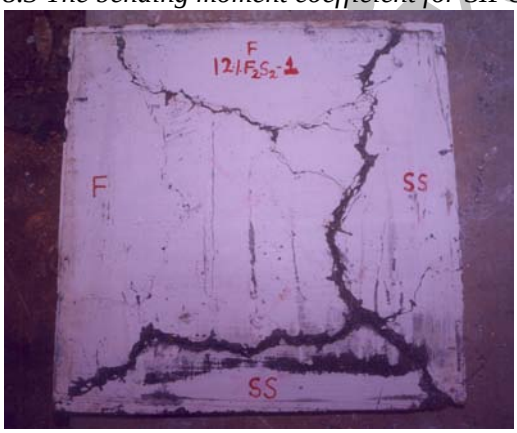

a. Experimental

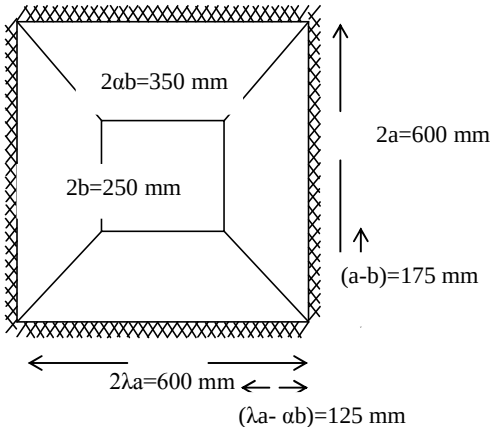

b. Idealized

Figure 19. Yield line pattern (SIFCON-12%)

From equation 3.

On substituting the above values in M_P equation we get

$$Mp = \frac{w(2a)^2}{24}\left[\frac{2\lambda + 2\alpha\frac{b^2}{a^2} + (\alpha+\lambda)\frac{b}{a}}{\left(1+\frac{Mp'}{Mp}\right)\left[\frac{\lambda a}{a-b} + \frac{a}{\lambda a - \alpha b}\right]}\right]$$

Note: $Mp = Mp'$

$$= \frac{w(2a)^2}{24}\left[\frac{2\ x1 + 2\,x1.213\,x\frac{125^2}{300^2} + (1.4+1)\ x\ \frac{125}{300}}{(1+\frac{1}{1})\left[\frac{1x\ 300}{(300-125)} + \frac{300}{(1x300 - 1.4x\ 125)}\right]}\right]$$

$$= \frac{w(2a)^2}{24}\left[\frac{2 + 0.486 + 1}{(2.00)(1.7142 + 2.4)}\right]$$

$= 0.176w\ (2a)^2$

$Mp = 0.0176\ w\ (2a)^2$

$Mp' = 0.0176\ w\ (2a)^2$

Therefore, the bending moment coefficient for SIFCON-12 is 0.0176

4. CONCLUSIONS

The major objective of this investigation is to produce SIFCON slabs with different volume fractions of fibres and test under uniformly distributed load. Cyclic load tests also have been performed. The superiority of SIFCON slabs over fibre reinforced concrete slabs and plain concrete slabs has been demonstrated. Analysing the results obtained from this investigation, the following conclusions are drawn.

- The load carrying capacity of the SIFCON slabs is much higher than the fibre reinforced concrete and plain concrete slab specimens.The increase of load carrying capacity of the SIFCON slab specimens is about 159%to 267% and 788 to 1166% with respect to FRC-2 and PCC-0 slab specimens respectively.
- The stiffness of SIFCON slabs is an order of higher magnitude than that of fibre reinforced concrete and plain concrete slab specimens.
- The SIFCON slab specimens exhibited greater ductility, even at the ultimate stage.
- Energy absorption increases with increase in fibre volume content in SIFCON slab specimens and the increase is steady from cycle to cycle.
- The increase of energy absorption capacity of SIFCON slab specimens is about 410 to 1066% and 9654 to 22202% when compared with FRC-2 and PCC-0 specimens respectively.
- The cumulative ductility factor increased almost five times for all SIFCON slab specimens from first cycle to fifth cycle.
- SIFCON slab specimens show superior performance than the FRC and PCC slab

specimens in flexure.

- Yield line analysis has been performed and Bending moment coefficient for different SIFCON slab are suggested.

REFERENCES

1. Lankard DR. Slurry infiltrated fiber concrete (SIFCON), *Concrete International*, **12**(1984) 44-7.
2. Lankard DR. Slurry infiltrated fiber concrete (SIFCON) properties and applications, Very high strength cement-based composites, *Material Research Society*, **42**(1985) 227-86.
3. Ghalib MA. Moment capacity of steel fibre reinforced small concrete slabs, *ACI Journal*, **77**(1980) 247-57.
4. Parameswaran VS, Krishnamoorthy TS, Balasubramanian K. Behaviour of high volume fibre cement mortar in flexure, *Cement and Concrete Composites* **12**(1990) 293-301.
5. Kumar V, Nautiyal BD, Choudhary RK. Yield line analysis of two way reinforced concrete slabs with corner opening-part-I: Derivations, *Journal of Structural Engineering ASCE*, **2**(2004) 125-37.
6. Craig RM, Sami HR, Gamil T, Brahim B. Flexural behaviour of one-way concrete slabs reinforced by fibre reinforced plastic reinforcements, *ACI Structural Journal*, **3**(1998) 353-65.
7. Marzouk H, Mohamed E, Sameh Hilal M. Effect of high-strength concrete slab on the behaviour of slab-column connections, *ACI Structural Journal*, **3**(1998) 227-37.
8. Aron Z. Yield line analysis of rectangular slabs with central openings, *ACI Journal*, **64**(1967) 838-44.
9. Ali RK, Majid A. Flexural behaviour of small steel fibre reinforced concrete slabs, *Cement and concrete composites* **27**(2005) 141-9.
10. Rao HS, Ramana NV. Behaviour of slurry infiltrated fibrous concrete (SIFCON) simply supported two-way slabs in flexure, *Indian Journal of Engineering and Materials Sciences*, **12**(2005) 427-33.
11. Abdullah R, Easterling WS. Determination of composite slab strength using new elemental test method, *ASCE Journal of Structural Engineering*, **133**(2007) 1268-77.
12. Muttoni A, Ruiz MF. Concrete cracking in tension members and application to deck slabs of bridges, *Journal of Bridge Engineering ASCE*, **12**(2007) 646-53.
13. Masood A, Arif M, Akthar S, Haquie M. Performance of ferrocement panels in different environments, *Cement and Concrete Research*, **33**(2003) 555-62.
14. Nayak SK, Menon D. Improved procedure for estimating short-term deflections in RC slabs, *Indian Concrete Journal*, **78**(2004) 19-25.